COMPARISON OF CLEAN-SC FOR 2D AND 3D SCANNING SURFACES 4TH BERLIN BEAMFORMING CONFERENCE

Mathew Legg*and Stuart Bradley†
Department of Physics, University of Auckland
Private Bag 92019, Auckland, New Zealand.

ABSTRACT

We present experimental data comparing the accuracy obtained for 2D and 3D scanning surfaces using CLEAN-SC deconvolution of beamformed acoustic maps. A spherical array is used to obtain recordings from a dense point cloud of sound source locations. Beamforming and CLEAN-SC acoustic maps are generated using traditional 2D scanning surfaces and 3D scanning surfaces corresponding to the surface geometry of an object being acoustically imaged. Results for the 3D method show improved accuracy of measured positions and magnitudes of sound sources under a range of circumstances. The most benefit, in regard to position error, is for frequencies above 5kHz and sound sources located less than a metre from the array. In these circumstances, the three-dimensionality is more dominant.

1 INTRODUCTION

Acoustic imaging using microphone phased array beamforming and deconvolution have traditionally used planar scanning surfaces to image the noise emitted by an object. This 2D scan surface is usually oriented perpendicular to the array's Z axis and located roughly at the same distance from the array as the object. This method is simple to use since the only information required to be known about the object is the approximate distance of the object from the array. Often, however, only a few of the scan points will correspond to the actual 3D surface of the object. This can cause incorrect focus (time delays) and spherical spreading correction being used for the beamforming. This can lead to errors in the resulting 2D beamforming and

*m.legg@auckland.ac.nz
†s.bradley@auckland.ac.nz

deconvolution maps which appear as incorrect measured sound pressure levels (*SPL*) and incorrect location of sound sources [5, 9, 11, 12]. There can also be parallax errors relating to the projection from the 2D map to the 3D object [8].

To address such issues, multiple planes forming a 3D grid of scan points have also been used for beamforming and deconvolution [3, 7, 13, 17] or similar acoustic imaging methods [14, 16]. Most of these scan points do not correspond to the surface geometry of the object. A problem encountered using this method, however, is that, for most practical arrays, the beamforming and deconvolution resolutions are poor in the direction along the array axis (longitudinal direction) compared to that in a direction parallel to the array (lateral direction) [3]. Also, these 3D grids can contain a large number of scan points which can make deconvolution of these 3D grid beamforming maps very computationally expensive.

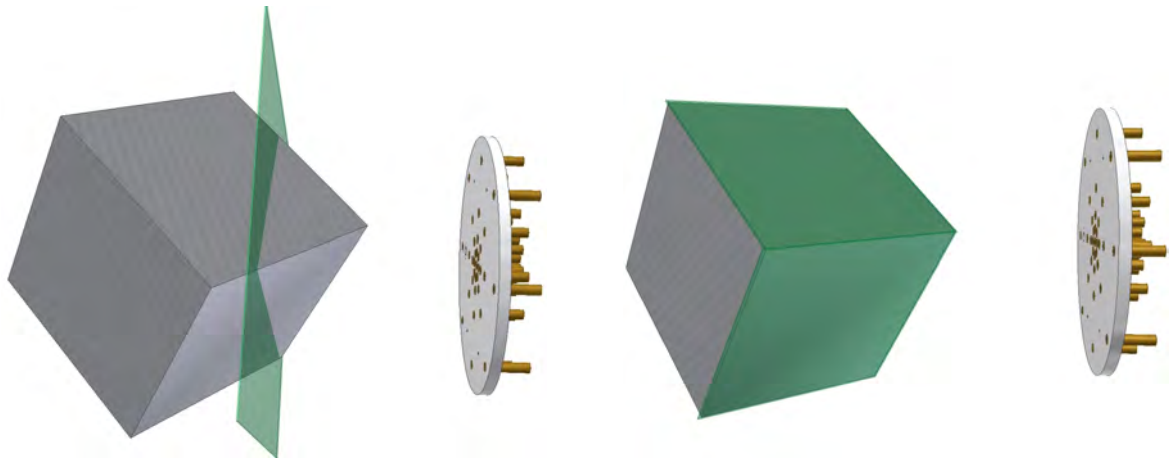

(a) Traditional 2D scanning surface.

(b) A 3D scanning surface corresponding to the surface of the object.

Figure 1: Illustration of a traditional 2D scanning surface and a 3D scanning surfaces corresponding to the surface geometry of the object for a SADA [10] microphone phased array.

An alternative technique that has been developed for beamforming is to use a scanning surface which corresponds to the 3D surface geometry of the object that is being acoustically imaged [1, 4, 9, 11, 12]. This method should provide more accurate beamforming focus (time delays), allow correction for spherical spreading to be made, and improved plotting accuracy by eliminating or reducing parallax effects. Experimental work using beamforming has shown this method can provide more accurate sound source magnitudes [5, 11, 12]. Improved accuracy of the localisation of sound sources using the 3D method is also mentioned in these works but no details on the magnitudes are provided. No detailed analysis comparing the position errors for 2D and 3D scanning surfaces for beamforming appears to have been previously carried out. Also, deconvolution of these 3D beamforming maps has not previously been performed. This paper presents experimental work which compares the magnitude and localisation accuracy obtained using beamforming and CLEAN-SC deconvolution for 2D and 3D scanning surfaces.

2 METHODOLOGY

2.1 Data Acquisition

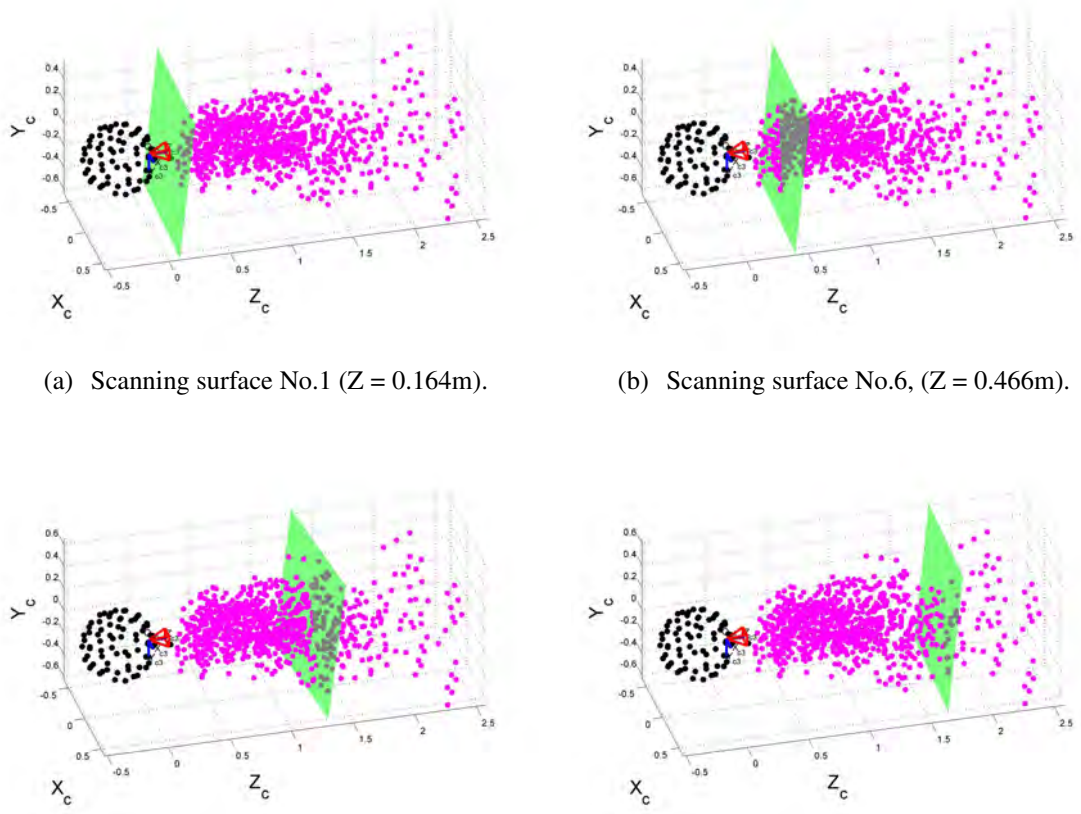

(a) Scanning surface No.1 (Z = 0.164m).

(b) Scanning surface No.6, (Z = 0.466m).

(c) Scanning surface No.15, (Z = 1.305m).

(d) Scanning surface No.19, (Z = 1.717m).

Figure 2: Illustration of several traditional planar scanning surfaces and the locations of the sound sources.

The sound source object used in this experiment was a piece of perspex or Lucite plastic which and had six 26mm diameter speakers inserted into its surface at set locations. These speakers have a relatively poor gain above 15kHz. The rig was setup on a tripod in front of a spherical 72 element, 0.6m dimeter microphone array. A new calibration technique (yet to be published) had been used to obtain the microphone coordinates $\vec{\boldsymbol{X}}_m$ in the reference frame of the array's camera. For each position and orientation of the speaker rig, nine microphone array recordings were made of white noise played on the speakers using simultaneously sampling, a sampling rate of 96 kSPS per channel, and a resolution of 16 bits. First, white noise was played on each of the six speakers in turn. Then white noise was played on four speakers simultaneously and then on all six speakers simultaneously. These white noise signals were generated using six analog outputs of the data acquisition hardware and different sequences in

a Kasami set and using an output sampling rate of 48kSPS. As a comparison, an additional recording was then made of uncorrelated white noise played on four speakers simultaneously using four microcontrollers with sperate clocks and on/off buttons. This process was repeated for 140 positions of the speaker rig. This gave a total of 1260 microphone recordings.

2.2 Data Processing

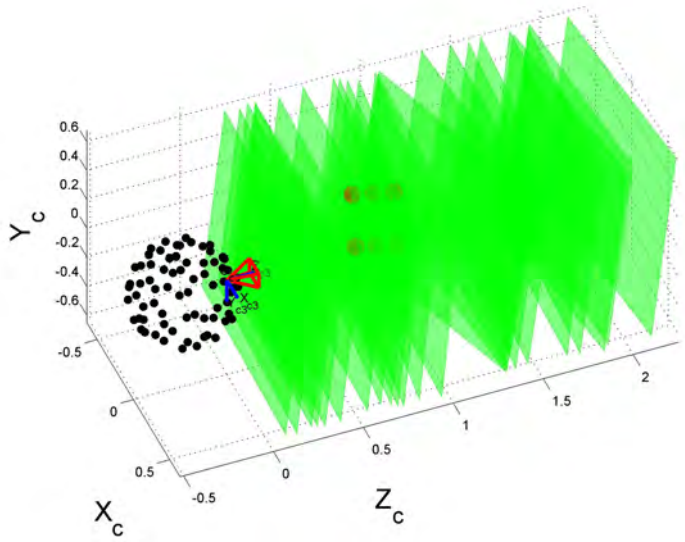

(a) Six speaker locations and 23 traditional 2D scanning surfaces.

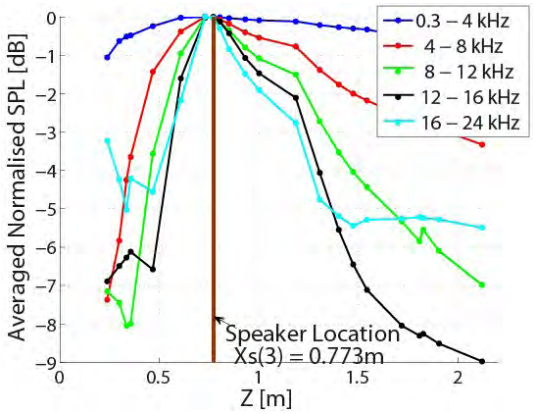

(b) Depth of field for a single speaker played (Record No.1).

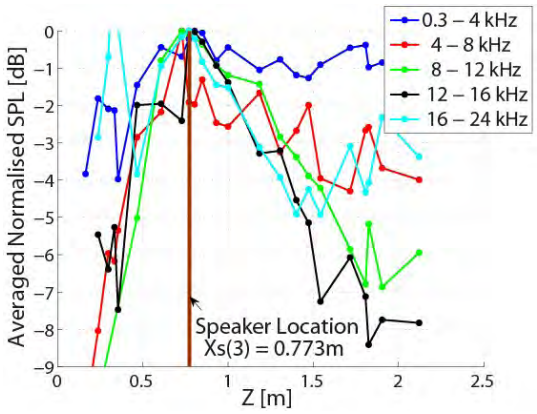

(c) Depth of field for six speakers played simultaneously (Record No.8).

*Figure 3: Plot showing the measured depth of field for 23 traditional 2D scanning surfaces at different distances from a spherical array corresponding to Speaker No.1, which was located at a distance of 0.773*m *from the array using normalised steering vectors.* (Speaker No.1, Image No.45, Traditional Image No.1-23.)

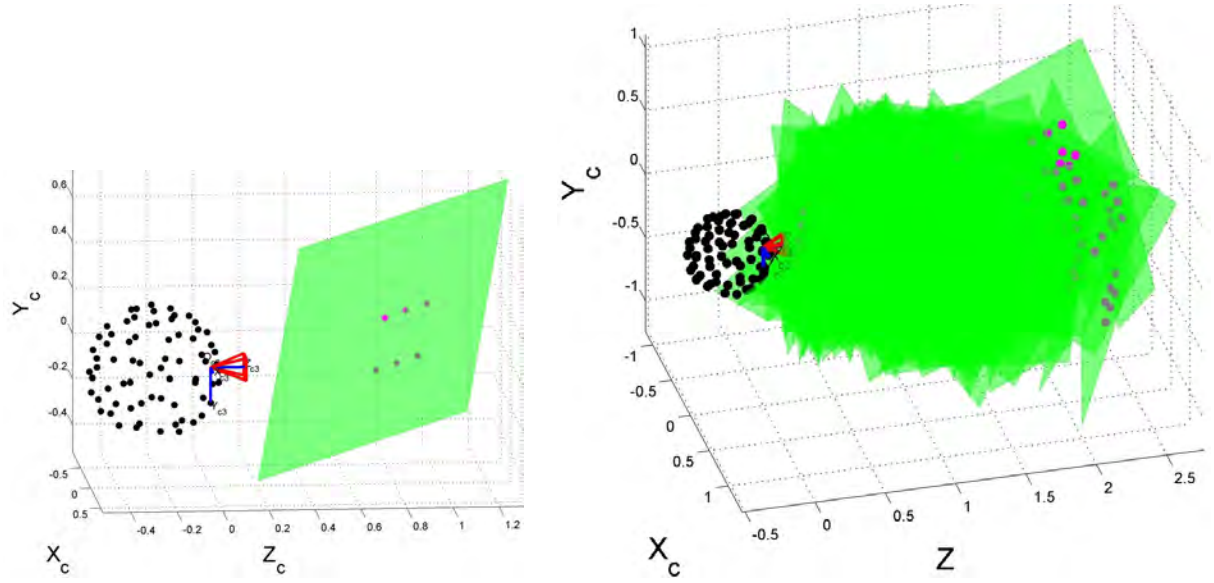

(a) A single 3D scanning surface passing through six sound sources.

(b) One hundred and forty 3D scanning surfaces each passing through six sound sources.

Figure 4: Illustration of the 3D scanning surfaces and the corresponding sound sources they pass through.

Using an automated process, frequency domain beamforming and *CLEAN-SC* deconvolution plots were then generated for each microphone array recording for both 2D and 3D scanning surfaces. The same methodology (yet to be published) was used to obtain both the 2D and 3D scanning surfaces. Cross spectral matrices $\mathbf{G}$ were then generated using a data block length K of 4096 samples, an overlap of data blocks of fifty percent, and a Hann window. The cross spectral matrices were then summed into twelfth octave frequency bands from 300Hz to 23kHz. These cross spectral matrices were then calibrated using Dougherty's eigenvalue calibration method [6]. A beamforming acoustic map $\boldsymbol{b}$ was then generated in each twelfth octave frequency band using

$$\boldsymbol{b}(\vec{\xi}_n) = \mathbf{w}^{\dagger}(\vec{\xi}_n)\ \mathbf{G}\ \mathbf{w}(\vec{\xi}_n), \quad \vec{\xi}_n = \vec{\xi}_1 \ldots \vec{\xi}_N \tag{1}$$

where $\vec{\xi}_n$ is the n^{th} scanning point coordinate and $\mathbf{w}$ is the array steering vector. The array steering vectors were initially calculated using

$$\mathrm{w}_m(\vec{\xi}_n) = \frac{\frac{e^{i\omega\|\vec{X}_m-\vec{\xi}_n\|/c}}{\|\vec{X}_m-\vec{\xi}_n\|}}{\sqrt{\sum_{m=1}^{M}\frac{1}{(\|\vec{X}_m-\vec{\xi}_n\|)^2}}}, \tag{2}$$

where ω is the angular frequency [2]. However, since they are normalised, they apply the same gain to each scan point and do not correct for spherical spreading. As a comparison, the steering vector

$$\mathrm{w}_m(\vec{\xi}_n) = \frac{1}{M}\,\|\vec{X}_m - \vec{\xi}_n\|\ e^{i\omega\|\vec{X}_m-\vec{\xi}_n\|/c}, \tag{3}$$

was also used. This is a slightly modified version of that given by Brooks and Humphreys [2, 10]. This gives a distance dependant weighting to each scan point and attempts to correct for spherical spreading.

Deconvolution of these beamforming maps was performed using *CLEAN-SC* [15]. Beamforming and *CLEAN-SC* were performed in an automatically process cycling through all recordings. For each *CLEAN-SC* map, the peak magnitudes $\boldsymbol{b}_{max}$ and their coordinates $\vec{\boldsymbol{\xi}}_{max}$ in the *CLEAN-SC* maps are obtained and used for error analysis. For a 3D scanning surface corresponding to the surface of the object, one could define the position error ε to be

$$\varepsilon = \|\vec{\boldsymbol{X}}_{\mathrm{s}} - \vec{\boldsymbol{\xi}}_{max}\|, \tag{4}$$

where $\vec{\boldsymbol{\xi}}_{max}$ is the deconvolution peak coordinate. However, if a 2D scanning surface is used, the scanning surface does not pass through a speaker coordinate $\vec{\boldsymbol{X}}_{\mathrm{s}}$. The deconvolution peaks were, therefore, projected from $\vec{\boldsymbol{\xi}}_{max}$ to a point $\vec{\boldsymbol{\xi}}_{p}$ in a plane perpendicular to the array axis at the same distance $Z = \vec{\boldsymbol{X}}_{\mathrm{s}}(3)$ as the speaker. The error may, therefore, be defined as

$$\varepsilon = \|\vec{\boldsymbol{X}}_{\mathrm{s}} - \vec{\boldsymbol{\xi}}_{p}\|. \tag{5}$$

Perspective projection from the center of the microphone coordinates was used. This position error method was used for both the 2D and 3D scanning surfaces.

3 RESULTS

3.1 Depth of Field

The depth of field of an array describes the reduction of the measured sound pressure level of a sound source as a traditional planar scanning surface is moved away from the true source location due to incorrect focus (time delays) being used. This was investigated for the spherical array using a single sound source and 23 traditional 2D scanning surfaces at different distances from the array, see Figure 3a. The CLEAN-SC depth of field, for sound played on only one speaker, is shown in Figure 3b. Since only one sound source is used, this is also equivalent to the beamforming depth of field. This plot shows a decrease in measured *SPL* as the traditional planar scanning surface was moved away from the true sound source location. This is consistent with the results obtained by [5, 11, 12] for beamforming. Figure 3c shows the CLEAN-SC depth of field for the same speaker but where all six speakers were played simultaneously. This plot shows similar results compared to the single speaker case but appears to have more noise.

3.2 Position Error

3.3 Scanning surfaces corresponding to the 3D surface geometry of the object

The CLEAN-SC position errors were then investigated for scanning surfaces corresponding to the 3D geometry of the object, see Figures 4a and 4b. In Figure 5, these position errors are averaged, for all speaker positions, into 12^{th} octave frequency bands. The position errors are high for low frequencies but reduce as the frequency is increased. For a single speaker played at a time, the mean position error is 3.7mm for the frequency the range 5-15kHz. This

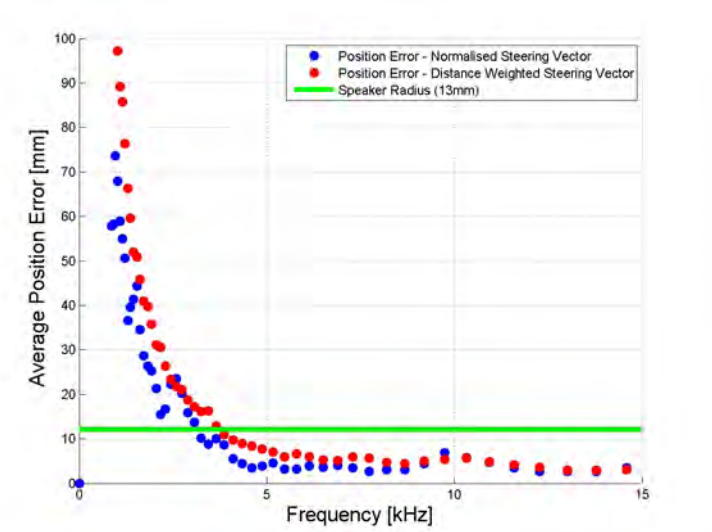

Figure 5: Clean-Sc position error averaged into 12^{th} *octave frequency bands for 3D scanning surfaces and sound played on only one speaker at a time. For frequencies from 5-15*kHz*, the position error is less than the diameter of the speaker.*

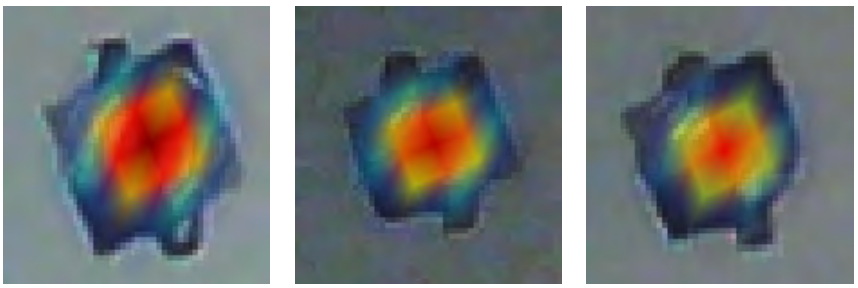

(a) (b) (c)

Figure 6: Example images of CLEAN-SC *peaks for speakers at a mean distance of 0.7*m *from the array using 3D scanning surfaces.*

error is remarkably small considering that the diameter of the speakers was 26mm and the scanning grid spacing used was 6mm. The poor performance at low frequencies was expected since beamforming resolution is proportional to wavelength. A plot of the position errors as a function of wavelength shows this linear relationship.

3.4 Comparison of position errors for 2D and 3D scanning surfaces

The CLEAN-SC position error was investigated as function of frequency for both the 2D and 3D case. The position error was averaged into octave frequency bands and plotted as a function of frequency for a white noise played on only a single speaker at a time, see Figure 7a and where sound was played on all six speakers simultaneously, see Figure 7b. At low frequencies, the position error for the 2D case was the same as that for the 3D case. However, the position

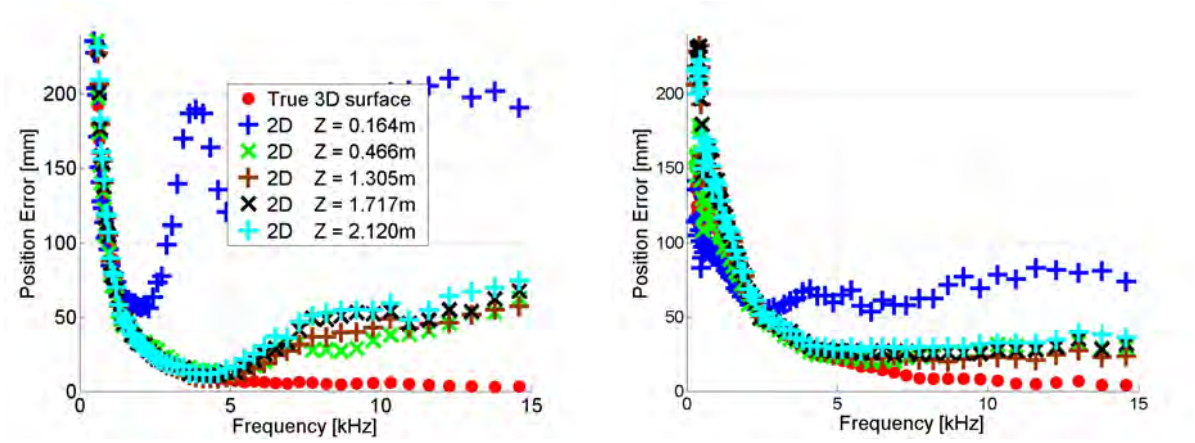

(a) White noise played on a single speakers (Record No.1-6).

(b) White noise played on multiple speakers simultaneously (Record No.8).

Figure 7: Position error averaged into 12^{th} *octave frequency bands.*

error for the traditional 2D scanning surfaces increased significantly above that of the 3D case for frequencies above 4.78kHz. An exception to this was for 2D scanning surface No.1 which departed from the 3D case at 1.4kHz.

The position error as a function of the Z component of the speaker positions was also investigated, see Figure 8. Here it can be seen that poor performance was achieved for 2D scanning surface No.1 and No.6 (Z= 0.164 and 0.466 m), for all speaker distances except for speaker coordinates near the 2D scanning plane. For 2D scanning surface No.15, No.19, and No.23 (Z= 1.305,1.717, and 2.120 m), the position error was comparable to the 3D case for speakers located further than about 0.8 to 1m from the array. An interesting feature observed when using a 3D scanning surface was that increased accuracy for lower frequencies was achieved as the sound was moved closer to the array. This was in contrast to the 2D case where high errors was observed for sound sources located near the array.

4 SUMMARY

The deconvolution algorithm *CLEAN-SC* was investigated using 3D scanning surfaces corresponding to the surface geometry of an object, and compared to results obtained for traditional 2D scanning surfaces. It was found that using 3D scanning surfaces corresponding to the surface geometry of an object gave under certain conditions large improvements in the accuracy of measured sound source magnitudes and positions compared to those obtained using the traditional 2D scanning surface. The greatest benefit of using the 3D scanning surface was achieved for higher frequencies and sound sources located near the array. Future work would repeat the experiment described above for the Underbrink multi-arm spiral array and the *SADA* array. The improvement in accuracy achieved for the spherical array using the 3D method is expected to be significantly greater for the Underbrink multi-arm spiral array, which has a shorter depth of field. Other deconvolution algorithms could also be investigated using the same methodology.

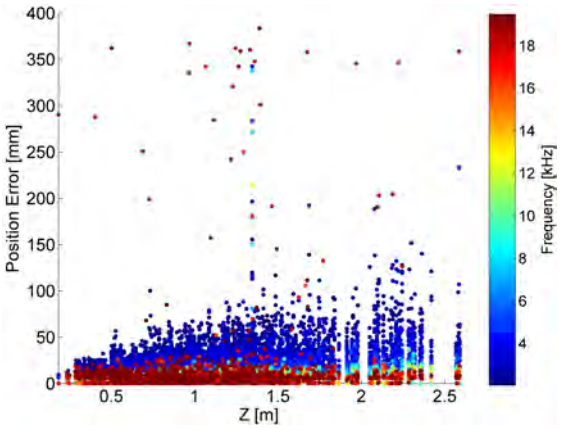

(a) True 3D scanning surface.

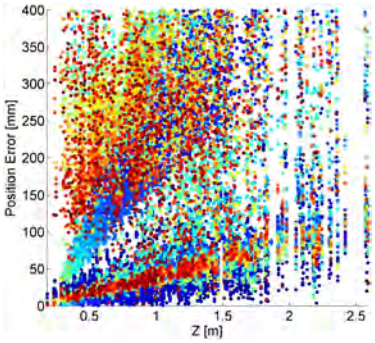

(b) Traditional 2D scanning surface No.1, Z = 0.164m.

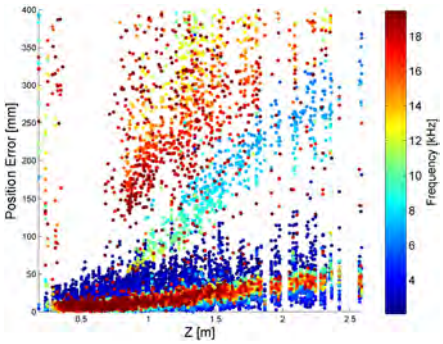

(c) Traditional 2D scanning surface No.6, Z = 0.466m.

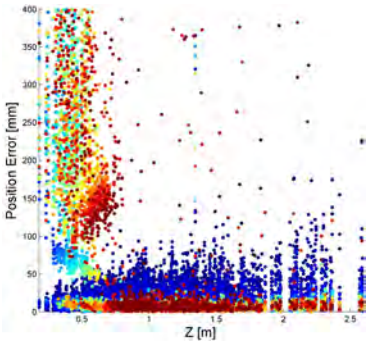

(d) Traditional 2D scanning surface No.15, Z = 1.305m.

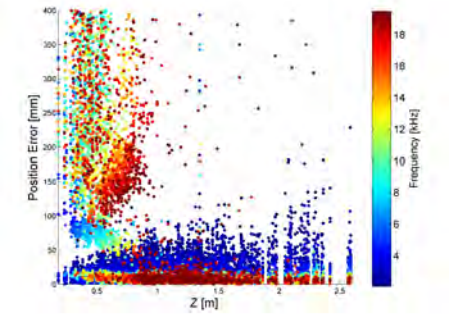

(e) Traditional 2D scanning surface No.19, Z = 1.717m.

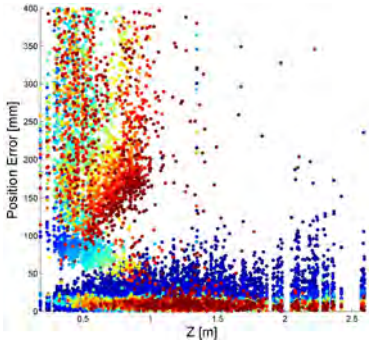

(f) Traditional 2D scanning surface No.23, Z = 2.120m.

*Figure 8: Comparison of position error as a function of distance Z from the array for the true 3D scanning surface and five traditional 2D scanning surface. The frequency range used was between 2 and 18*kHz*. The relatively poor position accuracy from 15 to 18*kHz *is related to the poor gain of the speaker at these higher frequencies. (Record No.1-6)*

,

References

[1] Bernard Béguet and Maxime Robin. Device for measuring and representing noise sources inside a space. Patent No. EP2182334 (A1), 5 May 2010.

[2] Thomas F. Brooks and William M. Jr. Humphreys. A deconvolution approach for the mapping of acoustic sources (DAMAS) determined from phased microphone arrays. In *10th AIAA/CEAS Aeroacoustics Conference*, Manchester, May 10-12 2004. AIAA-2004-2954.

[3] Thomas F Brooks and William M. Jr. Humphreys. Three-dimensional application of DAMAS methodology for aeroacoustic noise source definition. In *11th AIAA/CEAS Aeroacoustics Conference*, Monterey, CA, 2005. AIAA 2005-2960.

[4] Dirk Döbler, Gunnar Heilmann, Andy Meyer, and Mojtaba Navvab. Fields of application for three-dimensional microphone arrays for room acoustic purposes. Acoustic Camera - Newsletter: Edition 3, September 2011.

[5] Dirk Döbler, Gunnar Heilmann, and Ralf Schröder. Investigation of the depth of field in acoustic maps and its relation between focal distance and array design. In *Inter Noise 2008*, Shanghai, China, 26-29 October 2008.

[6] R. P. Dougherty. Beamforming in acoustic testing. In T. J. Mueller, editor, *Aeroacoustic Testing*, pages 63–97. Springer-Verlag, Berlin, 2002.

[7] R. P. Dougherty. Jet noise beamforming with several techniques. In *Berlin Beamforming Conference*, 24-25 February 2010.

[8] Robert P. Dougherty. Extensions of DAMAS and benefits and limitations of deconvolution in beamforming. In *11th AIAA/CEAS Aeroacoustics Conference (26th AIAA Aeroacoustics Conference)*, Monterey, California, 23 - 25 May 2005. AIAA 2005-2961.

[9] Gunnar Heilmann, Andy Meyer, and Dirk Döbler. Beamforming in the time-domain using 3d-microphone arrays. In *XIXth Biennial Conference of the New Zealand Acoustical Society*, Auckland, 2008.

[10] W M Humphreys, T F Brooks, W W Hunter, and K R Meadows. Design and use of microphones directional arrays for aeroacoustic measurements. In *36st AIAA Aerospace Sciences Meeting and Exhibit*, pages 98–0471, Reno, USA, 12-15 January 1998. AIAA 98-0471.

[11] C. Irimia, F. Deblauwe, K. Jannens, Z. Juhos, and S. Ignat. Improving the localization of noise sources inside a vehicle. *Scientific bulletin: automotive series, year XV*, B(19), 2009.

[12] M. Maffei and A. Bianco. Improvements of the beamforming technique in pininfarina full scale wind tunnel by using a 3d scanning system. *SAE International Journal of Materials and Manufacturing*, 1(1):154–168, 2008.

[13] Patricio A. Ravetta. *LORE Approach for Phased Array Measurements and Noise Control of Landing Gears*. PhD thesis, Virginia Polytechnic Institute and State University, Blacksburg, Virginia, 28 November 2005.

[14] Ennes Sarradj. Improving speed with orthogonal beamforming. In *3rd Berlin Beamforming Conference*, Berlin, 24 - 25 Feb 2010.

[15] Pieter Sijtsma. CLEAN based on spatial source coherence. Technical report, National Aerospace Laboratory NLR, 2007.

[16] Y Wang, J Li, P Stoica, M Sheplak, and T Nishida. Wideband RELAX and wideband CLEAN for aeroacoustic imaging. *Journal of the Acoustical Society of America*, 115(2): 757–767, 2004.

[17] A. Xenaki, F. Jacobsen, E. Tiana-Roig, and E. F. Grande. Improving the resolution of beamforming measurements on wind turbines. In *Proceedings of 20th International Congress on Acoustics, ICA*, Sydney, Australia, 23–27 August 2010.